prosthesis

MDPI

Article

Citric Acid-Based Solutions as Decontaminant Mouthwash in Titanium and Dental Prostheses Materials in Implantoplasty Processes

Pilar Fernández-Garrido [1], Pedro Fernández-Dominguez [2], Laura Fernández De La Fuente [1], Barbara Manso De Gustin [1], José Felipe Varona [2], Begoña M. Bosch [3], Javier Gil [3,*] and Manuel Fernández-Domínguez [2]

[1] Department of Translational Medicine, CEU San Pablo University, Urbanización Montepríncipe, 28925 Madrid, Spain; pilarfergarrido@gmail.com (P.F.-G.); laurafernandezdelafuente@gmail.com (L.F.D.L.F.); barbaramdeg@gmail.com (B.M.D.G.)

[2] Facultad de Odontología, Universidad Camilo José Cela, C/Castillo de Alarcón, 49. Urb. Villafranca del Castillo, 28691 Villanueva de la Cañada, Spain; pfernandezdominguez@gmail.com (P.F.-D.); jfvarona@hmhospitales.com (J.F.V.); clinferfun@yahoo.es (M.F.-D.)

[3] Bioengineering Institute of Technology, Facultad de Medicina y Ciencias de la Salud, Universitat Internacional de Catalunya, Josep Trueta S/n, 08195 Sant Cugat del Vallés, Spain; bbosch@uic.es

* Correspondence: xavier.gil@uic.es

Abstract: The machining of implants and parts for dental prostheses to eliminate biofilm in the implantoplasty process causes a loss of mechanical properties and also characteristics of the surfaces, making tissue regeneration difficult. In the present work, treatments consisting of elements that can reduce infection, such as citric acid and magnesium, together with elements that can improve cell adhesion and proliferation, such as collagen, are proposed for implant–crown assembly. Titanium, zirconia, composite (PMMA + feldspar) and cobalt–chromium discs were immersed in four different solutions: 25% citric acid, 25% citric acid with the addition of collagen 0.25 g/L, 25% citric acid with the addition of 0.50 g/L and the latter with the addition of 1% Mg $(NO_3)_2$. After immersion was applied for 2 and 10 min, the roughness was determined by interferometric microscopy and the contact angle (CA) was evaluated. Human fibroblastic and osteoblastic line cells (HFFs and SaOS-2) were used to determine cell viability and proliferation capacity. Cell binding and cytotoxicity were determined by resazurin sodium salt assay (Alamar Blue) and cell morphology by confocal assay (immunofluorescence F-actin (phalloidin)) after 3 days of incubation. For the evaluation of bacterial activity, the bacterial strains *Sptreptococcus gordonii* (Gram+) and *Pseudomonas aeruginosa* (Gram−) were used. The antibacterial properties of the proposed treatments were determined by means of the resazurin sodium salt (Alamar Blue) assay after 1 day of incubation. The treatments considerably decreased the contact angle of the treated samples with respect to the control samples. The treatments endowed the surfaces of the samples with a hydrophilic/super-hydrophilic character. The combination of elements proposed for this study provided cell viability greater than 70%; considering the absence of cytotoxicity, it therefore promotes the adhesion and proliferation of fibroblasts and osteoblasts. In addition, it also endows the surface with antibacterial characteristics against from Gram+ and Gram− bacteria without damaging the cells. These results show that this mouthwash can be useful in oral applications to produce a new passivation layer that favors the hydrophilicity of the surface and promotes cellular activity for the formation of fibroblasts and osteoblasts, as well as showing bactericidal activity.

Keywords: citric acid; fibroblasts; osteoblasts; wettability; bactericide effect; mouthwash

Citation: Fernández-Garrido, P.; Fernández-Dominguez, P.; Fernández De La Fuente, L.; Manso De Gustin, B.; Varona, J.F.; Bosch, B.M.; Gil, J.; Fernández-Domínguez, M. Citric Acid-Based Solutions as Decontaminant Mouthwash in Titanium and Dental Prostheses Materials in Implantoplasty Processes. *Prosthesis* **2024**, *6*, 1211–1227. https://doi.org/10.3390/prosthesis6050087

Academic Editors: Kelvin Ian Afrashtehfar and Marco Cicciu

Received: 9 August 2024
Revised: 21 September 2024
Accepted: 24 September 2024
Published: 10 October 2024

1. Introduction

Dental implants have emerged as the preferred solution for restoring both aesthetics and function lost due to missing teeth, given their high success rates [1–3]. However, along-

side the rising popularity of dental implants, there has been a corresponding increase in the occurrence of biological complications, in particular, peri-implantitis, a destructive biofilm-mediated inflammatory condition characterized by inflammation in the peri-implant connective tissue and progressive loss of supporting bone [4]. Currently, the main challenge in oral implantology is the bacterial infection of dental implants causing diseases such as periodontitis and peri-implantitis. This issue results in 24% of dental implants requiring revision within 10 years of implantation [4,5].

Given the infectious nature of this condition, the primary therapeutic goal is to modify the environment to promote an aerobic ecosystem, fostering health and stability. In order to accomplish this, it is vital to disrupt biofilm formation on the surface of the affected implant and to address any local factors that may have contributed to the onset and progression of the disease [5]. For this purpose, different surgical and non-surgical measures have been proposed.

One of the solutions is to replace the infected dental implant with a new one. However, in some cases, a calcium phosphate filling should be produced for bone regeneration, and once sufficient bone formation is achieved, the new implant should be placed [6,7]. In other situations, the removal of the infected implant does not allow for the placement of a new dental implant because there is not enough space [8,9]. This fact means that the clinician must extract neighboring teeth to achieve the placement of a new implant. In some cases, narrow dental implants can be placed to avoid the removal of a healthy tooth [9]. As can be seen, the techniques are complicated, expensive for the patient, and have long treatment times [10–13].

This fact makes implantoplasty, which consists of the mechanization of the dental implant and part of its connection with the prosthesis to eliminate biofilm, a viable treatment option. This approach avoids clinical complications but causes a loss in the mechanical properties of the implant and the prosthesis. In the case of metal components, it reduces corrosion resistance and increases the release of ions into the physiological environment [14–19]. Figure 1 shows the surfaces of dental implants and prostheses machined in order to remove biofilm.

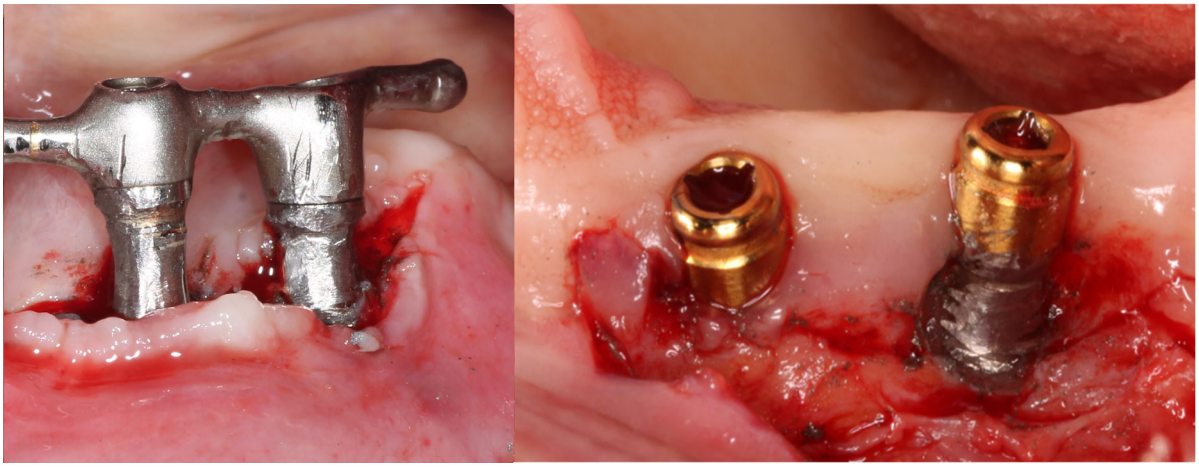

Figure 1. Dental implants and abutments treated by implantoplasty. Metallic particles in the tissue and grinding marks on the titanium surface produced by machining of the samples can be observed. These marks produce an increase in roughness.

Kotsakis et al. [20] demonstrated that the machining of titanium causes a reduction in oxygen concentration on the machined surface produced by the inflammation process, which degrades the protective titanium oxide layer (TiO_2) that acts as a passivation layer. Due to the lack of oxygen, pure titanium is formed and oxidized in a mixed way without reaching the stoichiometry of TiO_2. These so-called mixed oxides have lower corrosion

resistance and exhibit toxicity that hinders cellular activities, both in fibroblastic and osteoblastic functions [21,22].

Citric acid treatments, being weak acid treatments, do not chemically attack the titanium as more aggressive agents such as hypochlorous acid do. It has been observed that treatments with hypochlorous acid and hydrogen peroxide eliminate bacteria very effectively but cause a very significant increase in roughness that favors the rapid recolonization of bacteria. Other treatments, such as ozone gas, have been used but large doses cannot be given due to the risk of soft tissue necrosis. Similarly, strong acids are not suitable for oral treatment, as this acidic composition burns soft and hard tissues. For example, treatments with hydrofluoric acid react with apatites, generating fluorapatite crystals, which can cause severe pain to the patient [23,24]. These limitations have led to the consideration of citric acid as the best candidate to obtain mouthwashes for clinical application. In this research, citric acid solutions with weak pH are investigated in order to obtain a mouthwash solution. Beyond its bactericidal effect due to citric acid, it generates a titanium oxide layer approximately of 7 nanometers thick, which protects the dental implant from chemical degradation and electrochemical corrosion. This layer is homogeneous, compact and stoichiometric, leading to an increase in corrosion resistance and reduced ion release, as demonstrated by different authors [25,26]. Citric acid treatment favors the bactericidal character for different types of bacteria, both Gram-positive and Gram-negative. In order to improve cellular activity, different concentrations of collagen and divalent magnesium salts were added. These additions have been proven to increase cell adhesion, proliferation and differentiation [27–29]. The main goal of this research is to develop a solution that can be applied to patients undergoing implantoplasty, in order to mitigate or reduce the associated problems of this technique.

The hypothesis of this research is that citric acid solutions with collagen and magnesium cations will promote osteoblastic and fibroblastic cell behavior, presenting a bactericidal character in Gram-positive and Gram-negative bacteria.

2. Materials and Methods

2.1. Materials

For this study, 320 discs of 4 different materials were used in a dental implant system. The experimental design allowed for determining the number of samples, indicating 15 samples for each biological and microbiological test. The roughness and wettability studies did not affect the samples. The total was 60 but we incorporated 5 more per experiment for possible unforeseen events. This meant that there were 80 discs for each material:

- Ti: commercially pure Titanium (Ti), grade 3.
- Zr: zirconia (ZrO_2 with 2.5% in weight of yttria) (Y_2O_3).
- Composite formed by polymethyl methacrylate (PMMA) with feldspar $CaAl_2Si_2O_8$ with 38% in volume.
- CrCo: the chromium content was 30 wt%, the Mo content was 7 wt% and the W content was 0.1 wt%; cobalt was the balance.

Eighty discs for each material were supplied by the company SOADCO S.L. (SOADCO, Escaldes Engordany, Andorra).

Implantoplasty was carried out by the same researcher (JG) using the drilling protocol. To achieve this, a GENTLEsilence LUX 8000B turbine (KaVo Dental GmbH, Biberach an der Riß, Germany) under constant irrigation was used; the surface was sequentially modified with a fine-grained tungsten carbide bur (ref. number H379.314. 014 KOMET; GmbH & Co. KG, Lemgo, Germany). Tungsten carbide burs are the main tool for the initial shaping of implant prostheses, with the bur size adjusted to the specific area of treatment. Generally, larger burs are used on the vestibular and palatal sides, while smaller-diameter burs are employed in limited-access areas or interproximal spaces. These burs effectively eliminate implant threads, providing a smooth surface texture. Moreover, to create a refined finish, a series of polishing drills (from coarse- to fine-grained) are used. The references of the silicon carbide polishers are (order no. 9608.314.030 KOMET; GmbH & Co. KG, Lemgo,

Germany) for the coarse-grained and (order no. 9618.314.030 KOMET; GmbH & Co. KG, Lemgo, Germany) for the fine-grained [30–32]. The disks were sterilized at a temperature of 121 °C for 30 min.

The immersions were performed in four different dissolutions of chemical compositions, as shown in Table 1. The concentration proposed in this study were chosen because of different previous studies [25,26] that refer to passivation processes with citric acid and that do not cause irritation to soft tissues when applied. Also, the references on the effect of collagen and divalent cations, such as magnesium or calcium, made us introduce these elements in the formulation [23–26,28]. The different materials are immersed in the different solutions for 2 and 10 min. These times have been suggested by clinicians estimating between 2 and 10 min. These values are the most common in treatments with antibiotic agents and ozone treatments, among others, that are performed on the patient. Ten minutes is considered the maximum recommended value for the well-being of the patient.

Table 1. Citric-based dissolutions.

Dissolution	Chemical Composition
25% Citric acid (AC)	Citric acid 25% in volume (v)
25% Citric acid + collagen 250 (AC 250)	Citric acid 25% (v) with 0.25 g collagen/L
25% Citric acid + collagen 500 (AC 500)	Citric acid 25% (v) with 0.50 g collagen/L
25% Citric acid + collagen 500 + 1% Mg (AC 500/Mg)	Citric acid 25% (v) with 0.50 g collagen/L and 10% $Mg(NO_3)_2 \cdot 6H_2O$

2.2. Roughness Analysis

The smooth and micro-roughened surfaces were analyzed using a white light interferometer microscope (Wyko NT9300 Optical Profiler, Veeco Instruments, New York, NY, USA) in vertical scanning interferometry mode. A minimum of three measurements were taken from three different samples of each series. Approximately 230 imaging frames were used, enabling rapid and highly accurate measurements of the grooves. Surface analysis covered areas of 127.7 × 95.8 µm for groove imaging and 63.1 × 47.3 µm for plain regions within the grooves. Data filtering and analysis were conducted with Wyko Vision 4.10 software (Veeco Instruments), with a Gaussian filter applied to remove curvature and tilt from every surface analysis. Sa (average roughness) was measured, which represents the arithmetic average of the absolute values of the surface deviations from the mean plane [33–35].

2.3. Wettability

The contact angle (CA) was determined to evaluate the surface wettability of the titanium with treatments except the control for 2 and 10 min of immersion, using 5 samples per material. The wettability measurements of the samples were measured using the contact angle system "OCA 15 plus" (Dataphysics Instrument Company, Filderstadt, Germany) and the results were analyzed with "SCA20" software 123.45 (Dataphysics Instrument Company, Filderstadt, Germany).

For droplet deposition, a 1 mL "Braun" syringe was employed in a droplet generation system with micrometer displacement control, allowing for a precise dosing volume of 2 µL at a rate of 1 µL/s. The liquid droplets were backlit with LEDs through ground glass and the contact angle was measured 5 s after placing the droplets on the surface. MiliQ water was used for contact angle measurement, which was conducted on both untreated and treated samples with a "Citric Acid 25% + Collagen 500" solution after 2 and 10 min of immersion [36].

2.4. Fibroblast Culture

The objective of fibroblast cultures is to indicate the degree of cytocompatibility and the ease of regenerating soft tissue at the bone–soft tissue interface. This fact is of great importance for the formation of a biological seal to prevent bacterial leakage. Human

foreskin fibroblast (Millipore, Billerica, MA, USA) primary cells (HFFs) were cultured in phenol red-free Dulbecco's Minimum Essential Medium (DMEM; Invitrogen, Carlsbad, CA, USA) supplemented with 10% fetal bovine serum (FBS), L-glutamine (2 mM) and penicillin/streptomycin (50 U/mL and 50 mg/mL, respectively) at 37 °C in a humidified incubator at 5% CO_2, with media changed every 2 days. Cells between the sixth and tenth passages were used in all the experiments. Subconfluent cells were trypsinized, centrifuged and seeded at a density of 6×10^3 cells/disc with serum-free DMEM without phenol red onto different micro-grooved titanium discs in a 48-well microplate with an agarose layer (in order to prevent cell attachment to the dish). Tissue culture polystyrene (TCPS) and polished c.p. titanium served as reference substrates. Cellular analyses were performed at 4 h, 24 h and 72 h after seeding.

HFFs were cultured on the different surfaces. Then, cell adhesion and proliferation were analyzed using Cell Proliferation Reagent WST-1 (Roche Applied Science, Penzberg, Germany). This colorimetric protocol measures the creation of the formazan dye by cellular activity. The tetrazolium salts incorporated to the medium are cleaved by mitochondrial dehydrogenases of living cells, and the resulting soluble formazan dye can be analyzed spectrophotometrically. There is a direct correlation between the absorbance of the dye solution and the cell number. Viability was evaluated at the specified culture times by incubating for 2 h with 1:10 WST-1 in serum-free DMEM without phenol red. The optical density (OD) at 440 nm of cell supernatant was evaluated with an EL × 800 Universal Microplate Reader (Bio-Tek Instruments, Inc., Winooski, VT, USA). Three different samples for every surface and two different experiments were measured in parallel. A standard curve was performed using cell numbers ranging from 3×10^3 to 50×10^3.

Non-viable cells were quantified by means of measurement of released lactate dehydrogenase (LDH) enzyme at the specified culture times. For that purpose, the cell-free culture supernatant was collected, centrifuged at 250× *g* for 5 min and then analyzed with Cytotoxicity Detection Kit LDH (Roche Applied Science, Basel, Switzerland) as per the manufacturer's instructions. The reduction of tetrazolium salts into the formazan dye by LDH activity was measured spectrophotometrically at 490 nm. TCPS was used as a low control sample and lysed cells were utilized as a high control sample (maximum releasable LDH activity). Three different samples of each series in two experiments were analyzed.

2.5. Osteoblasts Culture

The objective of osteoblast cultures is to determine the degree of osteoblastic cytocompatibility and the ease of hard tissue regeneration to achieve bone regeneration and increase the mechanical fixation of the implant–abutment system to the bone with osseointegration. For the cell adhesion assay, osteoblastic SaOS-2 cells, a cell line with epithelial morphology derived from bone, were used. Six to seven cell passages were performed before seeding the cells onto the study samples. During cell passages, a control of the growth and cell viability was tested. Cells were initially thawed by gently shaking the cryovial in a 37 °C water bath for 1–2 min. From this point onward, everything was performed under sterile conditions. Once thawed, the content was transferred to a falcon with 9 mL of culture medium and centrifuged at 300 G for 3 min. Then, the supernatant was aspirated, and the pellet was resuspended with 1 mL of cell culture medium. Cells were seeded in flasks F175 and were kept at 37 °C with 5% CO_2, with the cell culture medium being changed 2–3 times per week.

The cell culture medium for this cell line consists of McCoy's 5a Medium Modified with L-glutamine 1.5 mM and 2200 mg/L sodium bicarbonate. This medium was supplemented with 15% fetal bovine serum (FBS), 1% penicillin/streptomycin (P/S) and 2% sodium pyruvate solution (NaPyr).

Cell passage was carried out at 90% confluence. Therefore, the cells were detached from the flasks by removing the medium, washing twice with 5 mL of PBS (37 °C) to remove dead cells, and then adding 5 mL of 0.05% trypsin. The flasks were left in the incubator at 37 °C with 5% CO_2 for 2–3 min. Afterward, trypsin was neutralized with

7 mL of cell culture medium (37 °C) and the content was transferred to a Falcon tube and centrifuged for 5 min at 300 G. The supernatant was then aspirated, and the pellet was resuspended with cell culture medium. Cell counting with Tripan Blue was then performed. For this, 10 µL of previously resuspended cells was prepared in an Eppendorf tube and mixed with Tripan Blue. A volume of 10 µL of the total was transferred to a Neubauer chamber for counting using phase contrast microscopy. The corresponding calculations were then carried out [37–39].

A resazurin salt assay (Alamar Blue) was used to assess cell proliferation and cell viability. The protocol was as follows: 5 mg resazurin salt (Sigma-Aldrich, St. Louis, MO, USA) was added to 1 mL of PBS, obtaining a stock solution of 5 mg/mL. Then, 100 µL was transferred to a Falcon tube with 50 mL of cell culture medium, and the solution was filtered to ensure sterile conditions. The final solution had a concentration of 10 µg/mL. This solution was protected from light.

After three days of cell culture, the culture medium was removed, and each well was washed with 500 µL of pre-warmed PBS. Then, 300 µL of 10 µg/mL resazurin solution was added in each well and incubated at 37 °C and 5% CO_2 for 3 h. Afterward, 200 µL from each well was transferred to a 96-well plate, transparent, and finally, the absorbance was analyzed. The wavelength was of 570 nm and 600 nm, and an Infinite® 200 PRO Multimode Absorbance Multimode Microplate Reader (TECAN, Männedorf, Switzerland) was used.

2.6. Immunofluorescence

For the immunofluorescence assay, a working solution of actin 488-stained phalloidin (100 nM) was prepared by diluting 58.8 µL of the 14 µM stock in 8.4 mL of PBS. Additionally, a DAPI solution was prepared by diluting 10 µL in 10 mL of PBS. Both solutions were kept at room temperature, without light exposure. A 0.1% Triton-X solution was made by diluting 1 mL of Triton-X in 9 mL of PBS. The samples were analyzed using the STELLARIS 5 Cryo Confocal Light Microscope.

After three days of cell culture, the culture medium was removed, and cells were washed with 500 µL of pre-warmed PBS. Then, 350 µL of 4% PFA/PBS was added in the wells at room temperature, in order to fix the cells. Following fixation, cells were washed with 500 µL of PBS and then permeabilization was performed using 350 µL of 0.1% Triton-X/PBS. After 10 min, the cells were washed with 500 µL of PBS and after, 350 µL of actin 488-stained phalloidin was incorporated.

Cells were then incubated for 30 min at room temperature without light exposure. After actin staining, cells were washed three times with 500 µL of PBS and cells were incubated with 350 µL of DAPI solution at room temperature in the dark for 2–3 min. Finally, they were washed again with 500 µL of PBS and cells were kept with 500 µL of PBS at 4 °C, without light exposure.

2.7. Bacterial Culture

Bacterial cultures were performed to determine the bactericidal capacity of the different solutions studied as a way to prevent bacterial recolonization. Gram+ and Gram− bacteria were used to see their behavior. The results give us important information for determining the best solution for oral application. We must take into account a limitation of this study, which is to determine the behavior with biofilm and not with isolated strains. In any case, the results allowed for us to characterize the bactericidal capacity of the solutions. Bacterial assays were performed using two oral pathogens, representing a Gram-negative and a Gram-positive bacterial strain. *Pseudomonas aeruginosa*, a Gram-negative bacterial strain, was sourced from Colección española de cultivos tipo (CECT 110, Valencia, Spain). For the Gram-positive strain, *Streptococcus gordonii* were used, and were obtained from Colección española de cultivos tipo (CECT 804, Valencia, Spain).

A total of six samples (n = 6) were used for the bacterial adhesion test, with three samples from each study group dedicated to the Gram-positive and three to the Gram-negative bacteria. Prior to the test, the culture media and material (PBS) were sterilized

by autoclaving at 121 °C for 30 min using autoclave oven SELECTA model Sterilmax (SELECTA, Abrera, Spain). As previously described, samples were also sterilized by incubating in alcohol three times for 5 min in sterile culture plates. Afterward, the samples were exposed to ultraviolet light for another 30 min [40–42].

Agar plates were incubated at 37 °C for 24 h. The bacterial inoculum was prepared by suspending the bacteria in 5 mL of Brain Heart Infusion Broth (BHI) (Sigma Aldrich, St. Louis, MO, USA) followed by an incubation for 24 h at 37 °C. The medium was then adjusted to an optical density of 0.1 at a wavelength of 600 nm (OD600 = 0.1). For the bacterial adhesion test, 500 µL of the suspension (OD600 = 0.1) was added to each well of the culture plate and incubated at 37 °C for 1 h, using an incubator oven MEMMERT BE500 (MEMMERT Gmbh, Scheabach, Germany). All tests were carried out under static conditions without external stirring.

Then, the samples were rinsed twice with PBS for 5 min each and fixed with a 2.5% glutaraldehyde solution in PBS for 30 min at 4 °C. Following fixation, the glutaraldehyde solution was removed, and the samples were rinsed three times with PBS for 5 min each.

For viability analysis, a confocal microscope and the LIVE/DEAD Backlight bacterial viability kit (Thermo Fisher, Barcelona, Spain) were used [35]. A solution was prepared by mixing 1.5 µL of propidium with 1 mL of PBS. Using a micropipette, a drop of this solution (approximately 50 µL/sample) was applied to the surface. After incubating at room temperature without light exposure for 15 min, the samples were rinsed three times with PBS for 5 min.

The surfaces were then examined by laser scanning microscopy (CLSM). Three images per sample were captured at 630× magnification. Live and dead bacteria were detected using a wavelength of 488 nm and 561 nm. This analysis enabled both the assessment of bacterial viability on each surface and an initial comparison of the of bacterial count present in the different group of samples.

2.8. Statistical Analysis

Statistical analysis was carried out using the comparative T.TEST (with the Excel software version 16.0.18025.20104). This was performed between the different groups at 95% of confidence. Therefore, statistically significant differences are with values of ($p < 0.05$).

3. Results

The roughness measurements (Sa) in Table 2, reveal that the different immersion treatments carried out on the discs increases slightly the roughness, as no statistically significant differences ($p < 0.05$) were observed with respect to the control group in Ti and Zr. However, regarding the roughness for Comp and CrCo, the implantoplasty produces higher roughness in relation to the control. In these cases, the differences are statistically significant $p < 0.05$.

Table 2. Roughness parameters values (Sa) in micrometers of the samples studied. The asterisks (*) mean differences statistically significant at $p < 0.05$ for each material and the different treatments. The double asterisks (**) mean differences statistically significant at $p < 0.05$ in relation to the values with single and without asterisks.

Treatment	Ti	Zr	Comp	CrCo
As-received	0.15 ± 0.09 *	0.10 ± 0.07	0.12 ± 0.09 *	0.18 ± 0.09 *
Implantoplasty (Ctrl)	0.25 ± 0.15 *	0.15 ± 0.05	0.28 ± 0.07 **	0.37 ± 0.10 **
AC	0.33 ± 0.13 **	0.17 ± 0.08	0.29 ± 0.09 **	0.40 ± 0.12 **
AC 250	0.30 ± 0.10 **	0.14 ± 0.09	0.27 ± 0.07 **	0.43 ± 0.13 **
AC 500	0.25 ± 0.11 **	0.17 ± 0.05	0.25 ± 0.08 **	0.44 ± 0.14 **
AC 500/Mg	0.27 ± 0.10 **	0.18 ± 0.04	0.26 ± 0.09 **	0.42 ± 0.15 **

From the roughness results, it can be observed that the implantoplasty generates a higher roughness than the control samples due to the machining processes (Table 1). Statistically significant differences can be seen in the surfaces with Ti implantoplasty when treated with the different citric acid solutions, since they present a slight acid attack that slightly increases the roughness values. For the other three materials used, the effect of immersion in the citric acid solution does not cause any statistically significant difference with the surface of the material that has undergone implantoplasty [32].

Figure 2 shows the results obtained from the surface contact angle measurements for each material treated with the different solutions for 2 and 10 min. First, the results obtained from the "Control" samples were only with implantoplasty treatment, but were only sterilized in an autoclave at 121 °C for 30 min. These values show values from 65° for composite to 99° for CrCo. These values show a considerable hydrophobic character. Of the four materials studied, the composite (PMMA) is the most hydrophilic material. On the other hand, the CrCo alloy has a hydrophobic surface because the contact angle is greater than 90°.

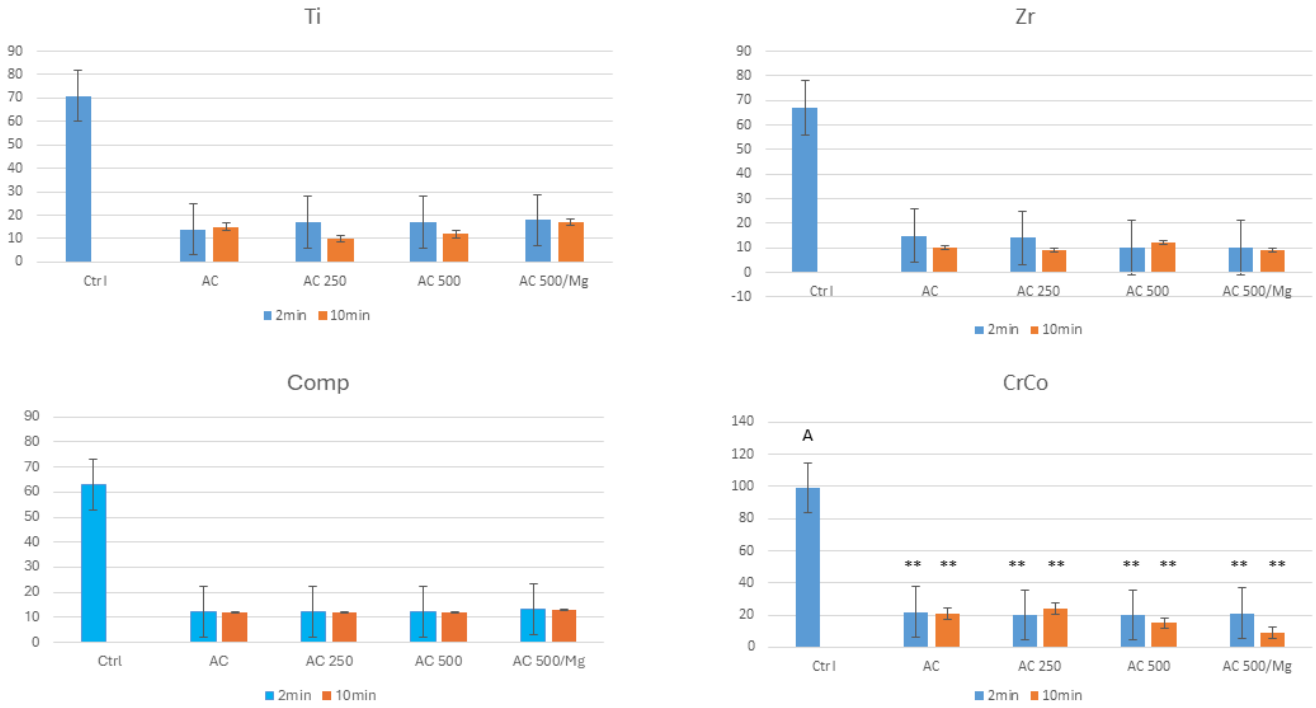

Figure 2. Contact angles of the different surfaces without treatment (Ctrl) and with immersion in different solutions based in citric acid studied. The samples were immersed for 2 and 10 min. The capital letter shows the statistical difference significance between CrCo, and the others surfaces with $p < 0.05$, and the asterisks the statistical difference significance between the immersion treatments of the CrCo and the other surfaces with $p < 0.05$. No statistical difference significance was found between the different times of treatment in any surface.

Secondly, the results obtained from the treated samples, i.e., immersed for 2 and 10 min in the citric acid solutions, show in all cases a very significant decrease in the contact angle, almost in all cases not exceeding 10° of contact angle, which makes the surfaces super-hydrophilic. The differences between the immersion times of 2 and 10 min do not show statistically significant differences ($p < 0.005$) in any of the treated materials. Moreover, no statistically significant differences are observed in the treated samples in general except in the case of CrCo. Specifically, CrCo values are around 20° while the other materials (Ti, Comp and Zr) present values around 10°.

Based on the results between 2 and 10 min, where no significant changes in behavior were observed, we focused this study on the two-minute immersion treatments. This

treatment time was selected because this solution is intended to function as a mouthwash, so the minimum time enhances patient comfort.

The results of the cell cytotoxicity test are presented in Figure 3 for the surface of the four proposed materials with the five conditions.

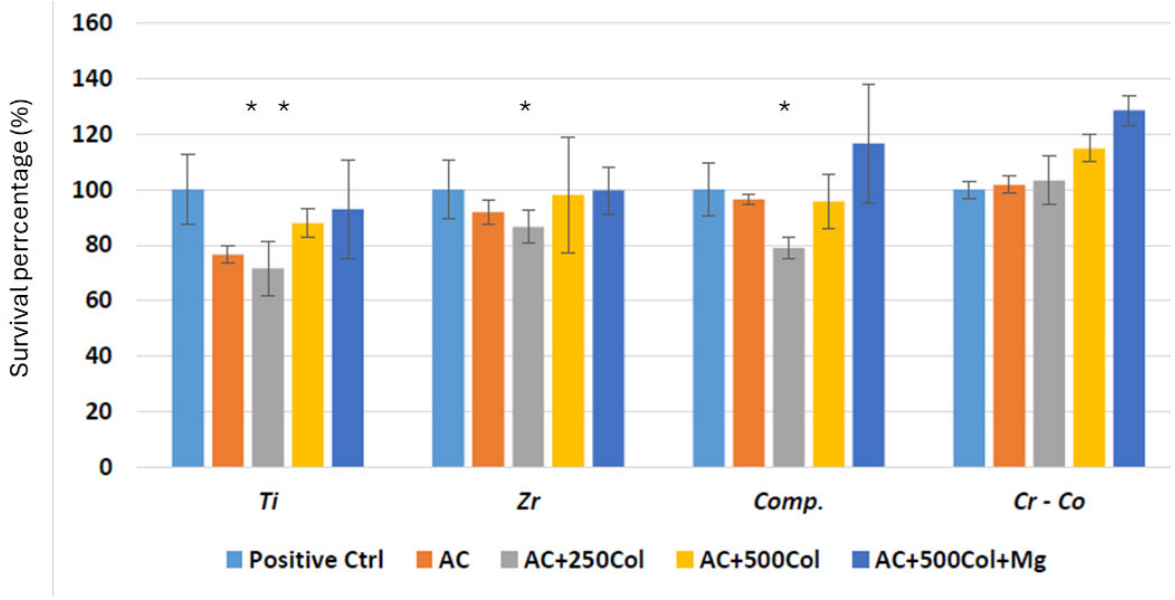

Figure 3. Survival percentage of fibroblasts for different treatments. Asterisks mean statistical differences significance $p < 0.05$.

Figure 3 shows that all citric acid treatments are cytocompatible, since the survival of the cultured fibroblast cells exceeds the 70% survival criterion. It can be seen that the AC + 500 Col and AC + 500 Col + Mg solutions show excellent behavior with fibroblasts.

Figure 4 demonstrates that collagen enhances the adhesion of fibroblasts, as more fibroblasts are present in this surface. The increase in collagen concentration does not offer statistically significant differences compared to the CrCo surface. However, it can be observed that there is a significant difference in the increase in the number of fibroblasts for the concentration of 500 in comparison to the lower concentration (250). No differences were observed between the other conditions studied.

An F-actin (phalloidin/DAPI) immunofluorescence assay was performed using a confocal light microscope in order to determine the presence and distribution of osteoblastic cells. This allowed for determining whether the material surfaces are favorable to the adhesion of this cells. Figure 5 shows that Ti and Zr surfaces show good cell viability for each treatment applied. Regarding the composite surfaces, treatments with 25% citric acid + 250 collagen and 25% citric acid + 500 collagen show a reduced number of cells, while the "Control" sample is the surface with the highest cell density. Regarding the CrCo surfaces, treatments with the 25% citric acid + 500 collagen and 25% citric acid + 500 collagen + 1% Mg present a decreased cell adhesion in comparison to the remaining surfaces.

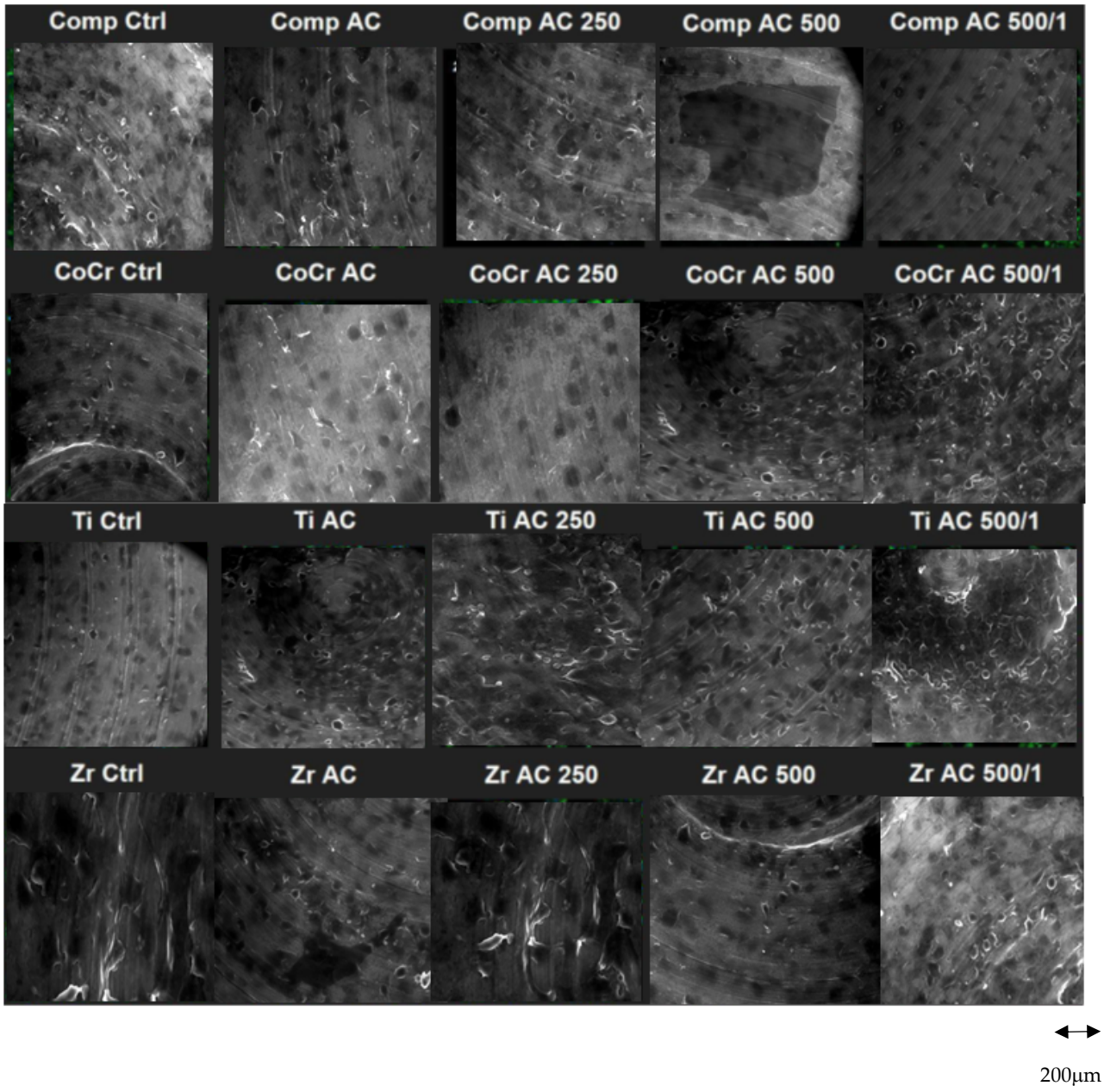

Figure 4. Fibroblasts cultured on different surfaces and with different dissolutions observed by scanning electron microscopy.

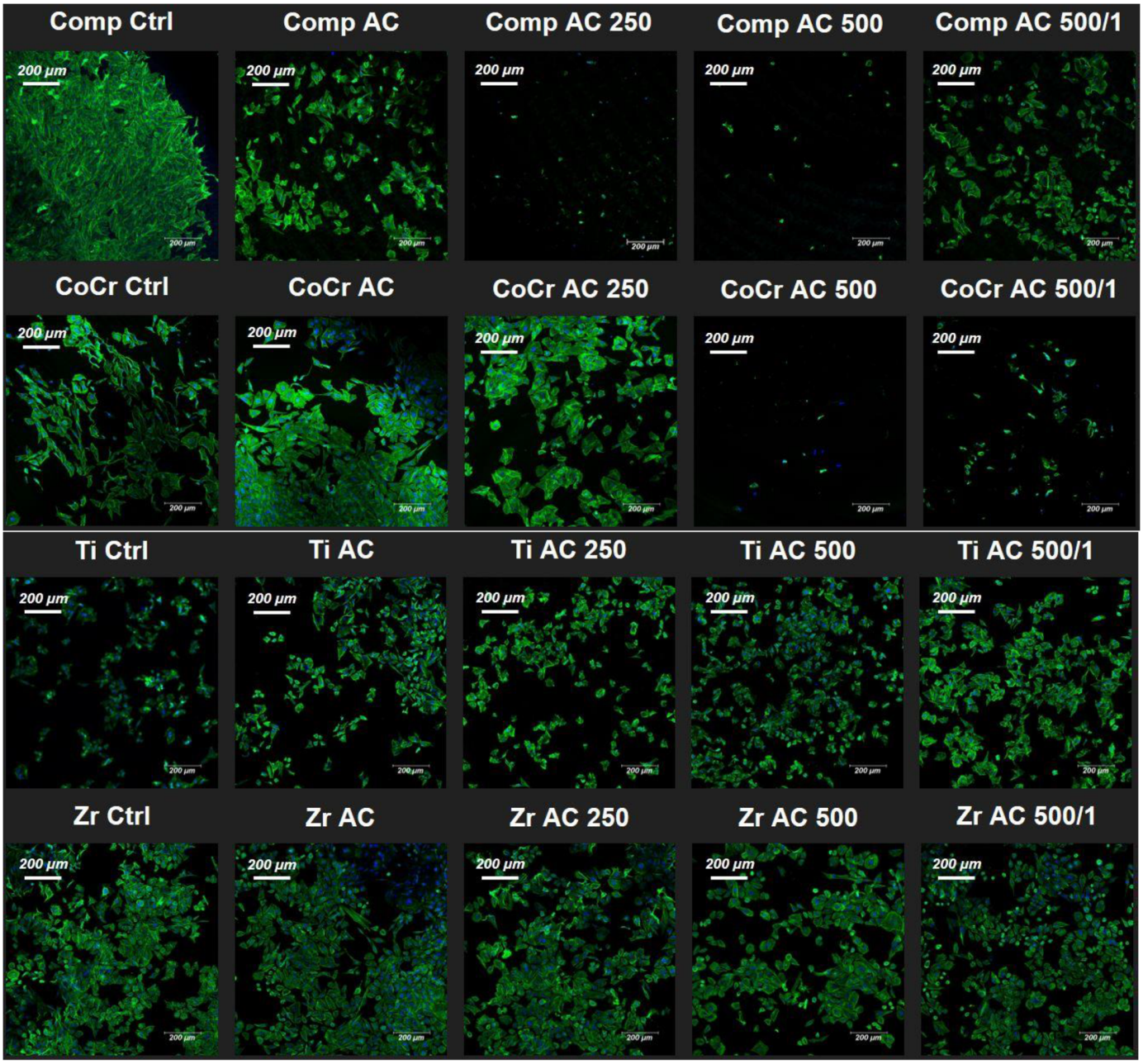

Figure 5. Immunofluorescence tests results of Ti, Zr, composite and CrCo surfaces with the applied treatments, showing the presence of osteoblastic cells.

Bacterial Culture

Figures 6 and 7 show the results obtained after the Alamar Blue test to determine the adhesion and bacterial growth on the surfaces proposed for the study for *Streptococcus gordonii* (Gram-positive) and *Pseudomonas aeruginosa* (Gram-negative). Significant bacterial colonization on all the surfaces in the control treatment can be observed, especially in the CrCo alloy. In all of them, both Gram-positive and Gram-negative bacteria show a notable reduction in bacterial activity when using citric acid treatments. It can be seen that the collagen and magnesium contents do not have a statistically significant effect on the reduction of bacterial colonization. It can also be seen that the action of citric acid with collagen causes a CFU reduction around of 75% for *Streptococcus gordonii* and 80% for *Pseudomonas aeruginosa*.

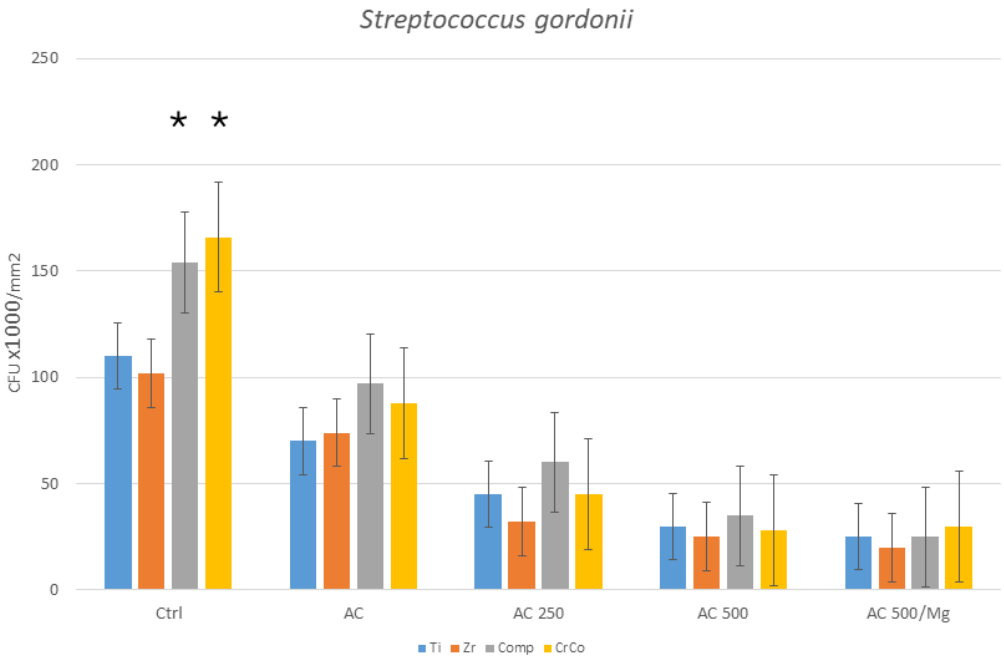

Figure 6. Quantitative analysis of *Streptococcus gordonii* (Gram+) for the different treatments and surfaces. Asterisks mean a statistically significant difference at $p < 0.05$. There are significant differences between the control and the four solutions studied for the materials studied. The different materials do not offer statistically significant differences with the treatments with the citric acid-based solutions and all of them offer important reductions in bacterial colonies. For the control samples, composite and CrCo present the worst bacterial behavior.

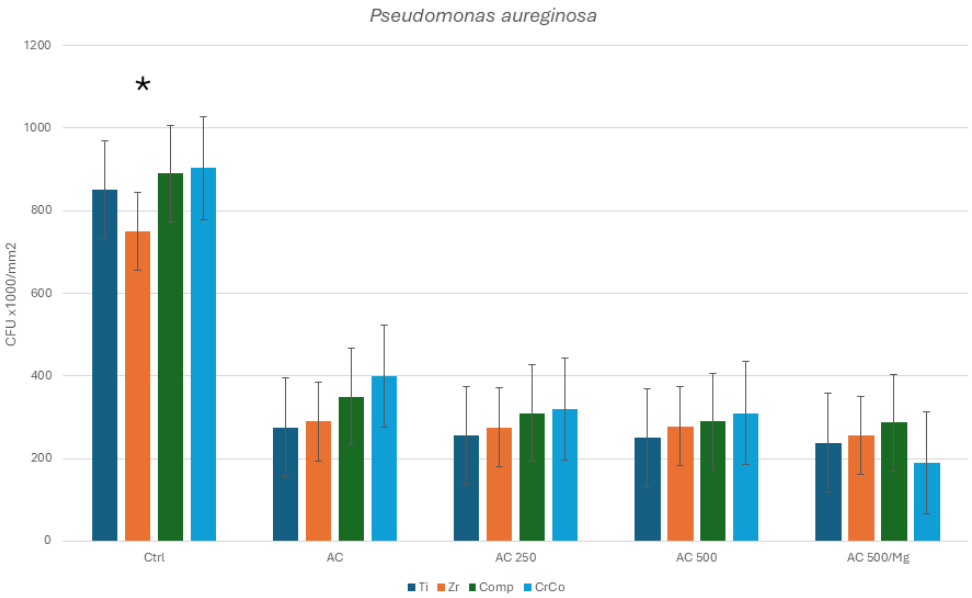

Figure 7. Quantitative analysis of *Pseudomonas aeruginosa* (Gram−) for the different treatments and surfaces. Asterisk means statistical differences significance $p < 0.05$. There are significant differences between the control and the four solutions studied for the materials studied in the colonies of Gram− bacteria. For the control samples, zirconia presents statistically significant differences with respect to the rest of the materials in relation to bacterial colonization. The different materials do not offer statistically significant differences among them with the treatments with the citric acid-based solutions and all of them offer significant reductions in bacterial colonies, but with a lower efficacy than for the Gram+ bacteria studied.

4. Discussion

It is well known that rough surfaces promote better cell adhesion, proliferation and differentiation, especially of osteoblastic cells [36,37]. Surface roughness or treated surfaces can interfere with cell morphology and orientation [38]. In this project, it is shown how the two metallic surfaces present greater roughness than the zirconia or the composite. It is also known that the increase in hydrophilicity favors wettability and, in consequence, this results in greater protein adsorption, which favors cell activity [43–46]. As has been observed, Ti presents higher wettability than CrCo, and therefore titanium has favorable factors for osteoblastic activity. Although CrCo surface exhibits good roughness, it has lower osteoblastic activity compared to Ti due to its low hydrophilic nature, which does not favor osteoblastic activity.

Based on the results obtained in the cell cytotoxicity test, it was determined that none of the treatments proposed for this study presented cytotoxicity for the SaOS-2 osteoblastic cells in any of the materials studied. Analyzing the values obtained, all of them are in the "non-cytotoxic" range, as determined by ISO 10993-5 [47]. The aforementioned ISO establishes that "the reduction of cell viability by more than 30% is considered a cytotoxic effect" [47]. Our results indicate a reduced adhesion of osteoblastic cells in the presence of collagen for the composite sample. This fact seems to be due to the lack of anchorage of the collagen molecules on the surface of the composite. This has been previously described by other authors, who concluded that the polymeric compound does not favor the adhesion of the collagen molecule and therefore inhibits the accelerating effect on both fibroblastic and osteoblastic cell adhesion [48,49].

Collagen is a well-known biomaterial commonly used in films, composites and three-dimensional matrixes, as it can enhance the recomposition and granulation of tissues, and also has the ability to act as protection of wounds and tissues against infection. Therefore, collagen is used as a support material in healing processes, and it is widely used in dental therapy. Moreover, it is a non-toxic, biodegradable and bioabsorbable material [32]. Also, collagen is the main component of ECM; type I is the most abundant, about 85%, together with proteins such as laminins, fibronectin and vitronectin. This fact favors cellular activity and should be a key element in triggering soft tissue formation to achieve a biological seal at the implant–abutment connection. In an in vivo study, Maria Sartori et al. investigated the effects of dental implants coated with type I collagen on bone regeneration and osseointegration in osteopenic rats, in which they found greater mechanical stability and a higher rate of osseointegration [50]. Other studies have affirmed the ability of type I collagen to promote osseointegration by stimulating bone formation at the cellular and molecular level [51]. In all cases, the collagen was dissolved in an acidic solution since it dissolves in an acid medium, which favors homogeneity and application.

The incorporation of magnesium is due to the fact that it has properties capable of improving bone bonding if implemented in implant surface modifications. It is currently used for titanium implant surfaces, providing improved properties. Jiang et al. were able to decrease Young's modulus, increase strength and provide improved biocompatibility in titanium implants. Veronese et al. combined titanium dioxide (TiO_2) with magnesium and obtained anti-inflammatory properties [52]. The inflammatory response plays an important role in the implantation of dental implants and may help to moderate osteogenesis [53,54].

The application of a citric acid treatment generates a small increase in surface roughness, which leads to an increase in bacterial adherence [55,56], but the acidic character provided to the sample surfaces prevents or decreases microbiological colonization [57]. The concentration of citric acid is related to the antibacterial action it provides, and thus causes a reduction in the pH of the extracellular matrices [23–26,28]. It is hypothesized that the presence of citric acid modifies the permeability of the bacterial membrane, varying the hydrogen gradient between intracellular and extracellular sites [52]. In addition, it has an antioxidant capacity to prevent or delay some type of cell damage and also has a negative effect on mycobacteria [52].

Focusing on the results of antibacterial activity obtained in Figures 5 and 6, it has been demonstrated that all treatments show antibacterial activity. In the case of pure titanium, in addition to the treatment provided, it is capable of forming a biocompatible titanium oxide layer, providing high resistance to corrosion with an oxidizing character, thus reducing bacterial activity [21,22,58].

A study has determined the existence of a relationship between wettability and bacterial colonization, based on the hydrophobicity of the surface [59,60]. For example, metallic surfaces that exhibit a hydrophobic nature result in a higher adhesion of hydrophobic bacteria. In consequence, lower bacterial adhesion could correlate with an increase in surface hydrophobicity [36,59]. Magnesium has also been shown to have an antibacterial effect, which could explain the lower levels of bacterial survival in Mg-containing samples, although the differences were not statistically significant [52,61].

Finally, of the four treatments studied, the one that stands out most for the osteointegrative and antibacterial properties provided is the Citric Acid 25% + Collagen 500 + Magnesium 1%. This has been validated by other studies that show how citric acid provides good antibacterial properties without damaging osteoblastic cells. Moreover, this is aligned with collagen and magnesium biological function, as collagen is the main component of the extracellular matrix capable of improving tissue recomposition, and magnesium improve bone union and presents antibacterial properties.

The action of citric acid in increasing surface hydrophilicity, producing a stable titanium oxide layer and bactericidal character improves systems based on strong acids or bases or ozone flux treatments. Firstly, because it does not improve the surface properties of titanium and in many cases, it affects its roughness or causes the incorporation of hydrogen into the titanium, which can cause the so-called hydrogen embrittlement. Moreover, in the case of treatment with citric acid-based solutions, it does not affect the health of the soft tissues. Finally, collagen can be dissolved in an acidic medium and can be incorporated into the solution in order to increase cell adhesion as well as to have a synergistic effect with divalent magnesium cations.

This work is preliminary but served in preparing cytocompatible citric acid-based solutions that favor both fibroblastic and osteoblastic cell activity and are clearly bactericidal against both Gram-positive and Gram-negative bacteria. However, concentrations should be optimized to improve cellular and bactericidal response. This study should be carried out in dental biofilm to complete the studies of two strains that are common in the mouth but do not respond reliably to what occurs in the mouth [62–65]. This study should be completed with in vivo studies with infection and to evaluate disinfection, as well as possible tissue regeneration in dental implants that have undergone implantoplasty. It is important to obtain a product that helps disinfection and favors bone growth for the new osseointegration of the implant, as well as the formation of a biological seal produced by the regeneration of the soft tissue [66,67]. Implantoplasty also faces other challenges such as the effect of the small particles, with different sizes and materials, that are present in the biological bed and present a toxic nature. Further studies should address this issue.

5. Conclusions

This contribution studies one of the most common materials in dental implant with prosthesis. The results verified the significant decrease in the contact angle for titanium, zirconia and PMMA composite with feldspar. Specifically, the values decreased from 70 to 15 and for CrCo from 100 to 25. All treatments showed that an increase in wettability causes higher cellular activity. Moreover, all treatments demonstrated cytocompatibility and good osteoblastic behavior. This suggests a promising solution for the regeneration of soft and hard tissues around the dental implant and the biological seal during prosthesis. It has been demonstrated that the different solutions have a strong bactericidal effect on both *Streptococcus gordonii* (Gram+) and *Pseudomonas aeruginosa* (Gram−) strains, reducing colonies around 72% and 64%, respectively. From the results obtained, the mouthwash with the best cellular activity and bactericidal capacity is the citric acid solution with

500 collagen and 1% magnesium. Although the in vitro results of this preliminary study are encouraging, further in vivo tests are needed before clinical application.

Author Contributions: Conceptualization, J.G., B.M.B. and M.F.-D.; methodology, P.F.-D., L.F.D.L.F., B.M.D.G. and J.F.V.; software, P.F.-G.; validation, J.G., P.F.-D., L.F.D.L.F., B.M.D.G. and J.F.V.; formal analysis, M.F.-D.; investigation, P.F.-G.; resources, M.F.-D.; data curation, P.F.-D., L.F.D.L.F., B.M.D.G. and J.F.V.; writing—original draft preparation, J.G. and B.M.B.; writing—review and editing, J.G.; visualization, M.F.-D.; supervision, J.G.; project administration, M.F.-D.; funding acquisition, M.F.-D. All authors have read and agreed to the published version of the manuscript.

Funding: This research received no external funding.

Institutional Review Board Statement: Not applicable.

Informed Consent Statement: Not applicable.

Data Availability Statement: The original contributions presented in this study are included in the article, further inquiries can be directed to the corresponding author.

Acknowledgments: The authors are grateful to Klockner Dental Implants. This work was supported by the Spanish Government and the Ministry of Science and Innovation of Spain through research projects CONCEPTO PDC2022-133628-C22 (co-funded by the European Regional Development Fund (ERDF), a way to build Europe) and research project MINECO (PID2022-137496OB-I00).

Conflicts of Interest: The authors declare no conflicts of interest.

References

1. Sailer, I.; Makarov, N.A.; Thoma, D.S.; Zwahlen, M.; Pjetursson, B.E. All-ceramic or metal-ceramic tooth-supported fixed dental prostheses (FDPs)? A systematic review of the survival and complication rates, Part I: Single crowns (SCs). *Dent. Mater.* **2015**, *31*, 603–623. [CrossRef]
2. Roos-Jansåker, A.M.; Lindahl, C.; Renvert, H.; Renvert, S. Nine- to fourteen-year follow-up of implant treatment, Part I: Implant loss and associations to various factors. *J. Clin. Periodontol.* **2006**, *33*, 283–289. [CrossRef]
3. Pjetursson, B.E.; Valente, N.A.; Strasding, M.; Zwahlen, M.; Liu, S.; Sailer, I. A systematic review of the survival and complication rates of zirconia-ceramic and metal-ceramic single crowns. *Clin. Oral Implant. Res.* **2018**, *29* (Suppl. S16), 199–214. [CrossRef]
4. Schwarz, F.; Derks, J.; Monje, A.; Wang, H.L. Peri-implantitis. *J. Periodont.* **2018**, *89* (Suppl. S1), S267–S290. [CrossRef]
5. Daubert, D.M.; Weinstein, B.F. Biofilm as a risk factor in implant treatment. *Periodontology 2000* **2019**, *81*, 29–40. [CrossRef]
6. Englezos, E.; Cosyn, J.; Koole, S.; Jacquet, W.; De Bruyn, H. Resective Treatment of Peri-implantitis: Clinical and Radiographic Outcomes After 2 Years. *Int. J. Periodontics Restor. Dent.* **2018**, *38*, 729–735. [CrossRef]
7. Romeo, E.; Lops, D.; Chiapasco, M.; Ghisolfi, M.; Vogel, G. Therapy of peri-implantitis with resective surgery. A 3-year clinical trial on rough screw-shaped oral implants. Part II: Radiographic outcome. *Clin. Oral Implant. Res.* **2007**, *18*, 179–187. [CrossRef]
8. Monje, A.; Schwarz, F. Principles of Combined Surgical Therapy for the Management of Peri-Implantitis. *Clin. Adv. Periodontics* **2022**, *12*, 57–63. [CrossRef]
9. Bertl, K.; Isidor, F.; von Steyern, P.V.; Stavropoulos, A. Does implantoplasty affect the failure strength of narrow and regular diameter implants? A laboratory study. *Clin. Oral Investig.* **2021**, *25*, 2203–2211. [CrossRef]
10. Leitão-Almeida, B.; Camps-Font, O.; Correia, A.; Mir-Mari, J.; Figueiredo, R.; Valmaseda-Castellón, E. Effect of bone loss on the fracture resistance of narrow dental implants after implantoplasty. An in vitro study. *Med. Oral Patol. Oral Cir. Bucal* **2021**, *26*, e611–e618. [CrossRef] [PubMed]
11. Hentenaar DF, M.; De Waal YC, M.; Stewart, R.E.; Van Winkelhoff, A.J.; Meijer HJ, A.; Raghoebar, G.M. Erythritol airpolishing in the non-surgical treatment of peri-implantitis: A randomized controlled trial. *Clin. Oral Implant. Res.* **2021**, *32*, 840–852. [CrossRef]
12. Tomasi, C.; Regidor, E.; Ortiz-Vigón, A.; Derks, J. Efficacy of reconstructive surgical therapy at peri-implantitis-related bone defects. A systematic review and meta-analysis. *J. Clin. Periodontol.* **2019**, *46* (Suppl. S21), 340–356. [CrossRef]
13. Schwarz, F.; Schmucker, A.; Becker, J. Efficacy of alternative or adjunctive measures to conventional treatment of peri-implant mucositis and peri-implantitis: A systematic review and meta-analysis. *Int. J. Implant. Dent.* **2015**, *1*, 22. [CrossRef]
14. Renvert, S.; Roos-Jansåker, A.M.; Claffey, N. Non-surgical treatment of peri-implant mucositis and peri-implantitis: A literature review. *J. Clin. Periodontol.* **2022**, *35* (Suppl. S8), 305–315. [CrossRef]
15. Monje, A.; Pons, R.; Amerio, E.; Wang, H.L.; Nart, J. Resolution of peri-implantitis by means of implantoplasty as adjunct to surgical therapy: A retrospective study. *J. Periodontol.* **2022**, *93*, 110–122. [CrossRef]
16. Barrak, F.N.; Li, S.; Muntane, A.M.; Jones, J.R. Particle release from implantoplasty of dental implants and impact on cells. *Int. J. Implant. Dent.* **2020**, *6*, 50. [CrossRef]
17. Toledano-Serrabona, J.; Sánchez-Garcés, M.A.; Gay-Escoda, C.; Valmaseda-Castellon, E.; Camps-Font, O.; Verdeguer, P.; Molmeneu, M.; Gil, F.J. Mechanical properties and corrosión behavior of Ti6Al4V particles obtained by Implatoplasty. An in vivo study. Part. II. *Materials* **2021**, *14*, 6519. [CrossRef]

18. Toledano-Serrabona, J.; Gil, F.J.; Camps-Font, O.; Valmaseda-Castellón, E.; Gay-Escoda, C.; Sánchez-Garcés, M.Á. Physicochemical and Biological Characterization of Ti6Al4V Particles Obtained by Implantoplasty: An In Vitro Study. Part I. *Materials* **2021**, *14*, 6507. [CrossRef]
19. Rupp, F.; Liang, L.; Geis-Gerstorfer, J.; Scheideler, L.; Hüttig, F. Surface characteristics of dental implants: A review. *Dent. Mater.* **2018**, *34*, 40–57. [CrossRef]
20. Kotsakis, G.A.; Lan, C.; Barbosa, J.; Lill, K.; Chen, R.; Rudney, J.; Aparicio, C. Antimicrobial Agents Used in the Treatment of Peri-Implantitis Alter the Physicochemistry and Cytocompatibility of Titanium Surfaces. *J. Periodontol.* **2016**, *87*, 809–819. [CrossRef]
21. Gil, F.J.; Planell, J.; Proubasta, I.; Vazquez, J. Fundamentos de biomecánica y biomateriales. In *Fundamentos de Biomecánica y Biomateriales*; Ergon: Barcelona, Spain, 1997; pp. 125–132.
22. Gil, F.J.; Planell, J.A. Aplicaciones biomédicas del titanio v sus aleaciones. *Biomecánica* **1993**, *1*, 34–43. [CrossRef]
23. Souza, J.G.S.; Cordeiro, J.M.; Lima, C.V.; Barão, V.A.R. Citric acid reduces oral biofilm and influences the electrochemical behavior of titanium: An in situ and in vitro study. *J. Periodontol.* **2019**, *90*, 149–158. [CrossRef] [PubMed]
24. Książek, E. Citric Acid: Properties, Microbial Production, and Applications in Industries. *Molecules* **2024**, *29*, 22. [CrossRef]
25. Cordeiro, J.M.; Pires, J.M.; Souza, J.G.S.; Lima, C.V.; Bertolini, M.M.; Rangel, E.C.; Barão, V.A.R. Optimizing citric acid protocol to control implant-related infections: An in vitro and in situ study. *J. Periodontal Res.* **2021**, *56*, 558–568. [CrossRef] [PubMed]
26. Fonseca, V.C.P.D.; Abreu, L.G.; Andrade, E.J.; Asquino, N.; Esteves Lima, R.P. Effectiveness of antimicrobial photodynamic therapy in the treatment of peri-implantitis: Systematic review and meta-analysis. *Lasers Med. Sci.* **2024**, *39*, 186. [CrossRef]
27. Wang, S.; Xu, C.; Yu, S.; Wu, X.; Jie, Z.; Dai, H. Citric acid enhances the physical properties, cytocompatibility and osteogenesis of magnesium calcium phosphate cement. *J. Mech. Behav. Biomed. Mater.* **2019**, *94*, 42–50. [CrossRef]
28. Brynhildsen, L.; Rosswall, T. Effects of cadmium, copper, magnesium, and zinc on the decomposition of citrate by a *Klebsiella* sp. *Appl. Environ. Microbiol.* **1989**, *55*, 1375–1379. [CrossRef]
29. Gil, F.J.; Solano, E.; Pena, J.; Engel, E.; Mendoza, A.; Planell, J.A. Microstructural, mechanical and citotoxicity evaluation of different NiTi and NiTiCu shape memory alloys. *J. Mater. Sci. Mater. Med.* **2004**, *15*, 1181–1185. [CrossRef]
30. Janson, O.; Gururaj, S.; Pujari-Palmer, S.; Karlsson Ott, M.; Strømme, M.; Engqvist, H. Titanium surface modification to enhance antibacterial and bioactive properties while retaining biocompatibility. *Mater. Sci. Eng. C* **2019**, *96*, 272–279. [CrossRef]
31. Costa-Berenguer, X.; Garcia-Garcia, M.; Sanchez-Torres, A.; Sanz-Alonso, M.; Figueiredo, R.; Valmaseda-Castellon, E. Effect of implantoplasty on fracture resistance and surface roughness of standard diameter dental implants. *Clin. Oral Implant. Res.* **2018**, *29*, 46–54. [CrossRef]
32. Francis, S.; Iaculli, F.; Perrotti, V.; Piattelli, A.; Quaranta, A. Titanium Surface Decontamination: A Systematic Review of In Vitro Comparative Studies. *Int. J. Oral Maxillofac. Implant.* **2022**, *37*, 76–84. [CrossRef] [PubMed]
33. Martin, J.Y.; Schwartz, Z.; Hummert, T.W.; Costochondral Schraub, D.M.; Simpson, J.; Lankford, J., Jr.; Dean, D.D.; Cochran, D.L.; Boyan, B.D. Effect of titanium surface roughness on proliferation, differentiation, and protein synthesis of human osteoblast-like cells (MG63). *J. Biomed. Mater. Res.* **1995**, *29*, 389–401. [CrossRef] [PubMed]
34. Boyan, B.D.; Lincks, J.; Lohmann, C.H.; Sylvia, V.L.; Cochran, D.L.; Blanchard, C.R.; Dean, D.D.; Schwartz, Z. Effect of surface roughness and composition on chondrocytes is dependent on cell maturation state. *J. Orthop. Res.* **1999**, *17*, 446–457. [CrossRef]
35. Godoy-Gallardo, M.; Guillem-Marti, J.; Sevilla, P.; Manero, J.M.; Gil, F.J.; Rodriguez, D. Anhydride-functional silane immobilized onto titanium surfaces induces osteoblast cell differentiation and reduces bacterial adhesion and biofilm formation. *Mater. Sci. Eng. C Mater. Biol. Appl.* **2016**, *59*, 524–532. [CrossRef]
36. Rabel, K.; Kohal, R.J.; Steinberg, T.; Tomakidi, P.; Rolauffs, B.; Adolfsson, E.; Palmero, P.; Fürderer, T.; Altmann, B. Controlling osteoblast morphology and proliferation via surface micro-topographies of implant biomaterials. *Sci. Rep.* **2020**, *10*, 12810. [CrossRef]
37. Esposito, M. Titanium for Dental Implants (I). In *Titanium in Medicine: Material Science, Surface Science, Engineering, Biological Responses and Medical Applications*; Brunette, D.M., Tengvall, P., Textor, M., Thomsen, P., Eds.; Springer: Berlin/Heidelberg, Germany, 2001.
38. Charest, J.L.; Eliason, M.T.; García, A.J.; King, W.P. Combined microscale mechanical topography and chemical patterns on polymer cell culture substrates. *Biomaterials* **2006**, *27*, 2487–2494. [CrossRef]
39. Mustafa, K.; Wennerberg, A.; Wroblewski, J.; Hultenby, K.; Lopez, B.S.; Arvidson, K. Determining optimal surface roughness of TiO(2) blasted titanium implant material for attachment, proliferation and differentiation of cells derived from human mandibular alveolar bone. *Clin. Oral Implant. Res.* **2001**, *12*, 515–525. [CrossRef]
40. Fielding, G.A.; Roy, M.; Bandyopadhyay, A.; Bose, S. Antibacterial and biological characteristics of silver containing, and strontium doped plasma sprayed hydroxyapatite coatings. *Acta Biomater.* **2012**, *8*, 3144–3152. [CrossRef] [PubMed]
41. Yamaguchi, S.; Nath, S.; Sugawara, Y.; Divakarla, K.; Das, T.; Manos, J.; Chrzanowski, W.; Matsushita, T.; Kokubo, T. Two-in-one biointerfaces—Antimicrobial and bioactive nanoporous gallium titanate layers for titanium implants. *Nanomaterials* **2017**, *7*, 229. [CrossRef]
42. Godoy-Gallardo, M.; Manzanares-Céspedes, M.C.; Sevilla, P.; Nart, J.; Manzanares, N.; Manero, J.M.; Gil, F.J.; Boyd, S.K.; Rodríguez, D. Evaluation of bone loss in antibacterial coated dental implants: An experimental study in dogs. *Mater. Sci. Eng. C Mater. Biol. Appl.* **2016**, *69*, 538–545. [CrossRef]
43. Medvedev, A.E.; Neumann, A.; Ng, H.P.; Lapovok, R.; Kasper, C.; Lowe, T.C. Combined effect of grain refinement and surface modification of pure titanium on the attachment of mesenchymal stem cells and osteoblast-like SaOS-2 cells. *Mater. Sci. Eng. C* **2017**, *71*, 483–497. [CrossRef] [PubMed]

44. Tao, Z.S.; Zhou, W.S.; He, X.W.; Liu, W.; Bai, B.L.; Zhou, Q. A comparative study of zinc, magnesium, strontium-incorporated hydroxyapatite-coated titanium implants for osseointegration of osteopenic rats. *Mater. Sci. Eng. C* **2016**, *62*, 226–232. [CrossRef]
45. Mitchel, J.A.; Hoffman-Kim, D. Cellular scale anisotropic topography guides Schwann cell motility. *PLoS ONE* **2011**, *6*, e24316. [CrossRef]
46. Huang, Q.; Elkhooly, T.A.; Liu, X.; Zhang, R.; Yang, X.; Shen, Z.; Feng, Q. Effects of hierarchical micro/nano-topographies on the morphology, proliferation and differentiation of osteoblast-like cells. *Colloids Surf. B Biointerfaces* **2016**, *145*, 37–45. [CrossRef]
47. *ISO 10993—5 (55)*; Biological Evaluation of Medical Devices—Part 5, Tests for In Vitro Cytotoxicity. ISO: Geneva, Switzerland, 2009.
48. Bax, D.V.; Smalley, H.E.; Farndale, R.W.; Best, S.M.; Cameron, R.E. Cellular response to collagen-elastin composite materials. *Acta Biomater.* **2019**, *86*, 158–170. [CrossRef]
49. Yoon, B.H.; Kim, H.W.; Lee, S.H.; Bae, C.J.; Koh, Y.H.; Kong, Y.M.; Kim, H.E. Stability and cellular responses to fluorapatite-collagen composites. *Biomaterials* **2005**, *26*, 2957–2963. [CrossRef]
50. Sartori, M.; Giavaresi, G.; Parrilli, A.; Ferrari, A.; Aldini, N.N.; Morra, M.; Cassinelli, C.; Bollati, D.; Fini, M. Collagen type I coating stimulates bone regeneration and osteointegration of titanium implants in the osteopenic rat. *Int. Orthop.* **2015**, *39*, 2041–2052. [CrossRef]
51. Kämmerer, P.W.; Scholz, M.; Baudisch, M.; Liese, J.; Wegner, K.; Frerich, B.; Lang, H. Guided Bone Regeneration Using Collagen Scaffolds, Growth Factors, and Periodontal Ligament Stem Cells for Treatment of Peri-Implant Bone Defects In Vivo. *Stem Cells Int.* **2017**, *2017*, 3548435. [CrossRef]
52. Veronese, N.; Pizzol, D.; Smith, L.; Dominguez, L.J.; Barbagallo, M. Effect of Magnesium Supplementation on Inflammatory Parameters: A Meta-Analysis of Randomized Controlled Trials. *Nutrients* **2022**, *14*, 679. [CrossRef]
53. Buser, D.; Schenk, R.K.; Steinemann, S.; Fiorellini, J.P.; Fox, C.H.; Stich, H. Influence of surface characteristics on bone integration of titanium implants. A Histomorphometric Study Miniat. *Pigs. J. Biomed. Mater. Res.* **1991**, *25*, 889–902. [CrossRef]
54. Schwarz, F.; Sahm, N.; Becker, J. Combined surgical therapy of advanced peri-implantitis lesions with concomitant soft tissue volume augmentation. A case series. *Clin. Oral Implant. Res.* **2014**, *25*, 132–136. [CrossRef] [PubMed]
55. Cochis, A.; Azzimonti, B.; Della Valle, C.; De Giglio, E.; Bloise, N.; Visai, L.; Cometa, S.; Rimondini, L.; Chiesa, R. The effect of silver or gallium doped titanium against the multidrug resistant Acinetobacter baumannii. *Biomaterials* **2016**, *80*, 80–95. [CrossRef]
56. Avila, G.; Misch, K.; Galindo-Moreno, P.; Wang, H.L. Implant surface treatment using biomimetic agents. *Implant. Dent.* **2009**, *18*, 17–26. [CrossRef]
57. Buxadera-Palomero, J.; Calvo, C.; Torrent-Camarero, S.; Gil, F.J.; Mas-Moruno, C.; Canal, C.; Rodríguez, D. Biofunctional polyethylene glycol coatings on titanium: An in vitro-based comparison of functionalization methods. *Colloids Surf. B Biointerfaces* **2017**, *152*, 367–375. [CrossRef]
58. Gosau, M.; Hahnel, S.; Schwarz, F.; Gerlach, T.; Reichert, T.E.; Bürgers, R. Effect of six different peri-implantitis disinfection methods on in vivo human oral biofilm. *Clin. Oral Implant. Res.* **2010**, *21*, 866–872. [CrossRef]
59. Zhang, X.; Bai, R.; Sun, Q.; Zhuang, Z.; Zhang, Y.; Chen, S.; Han, B. Bio-inspired special wettability in oral antibacterial applications. *Front. Bioeng. Biotechnol.* **2022**, *10*, 1001616. [CrossRef]
60. Hemmatian, T.; Lee, H.; Kim, J. Bacteria Adhesion of Textiles Influenced by Wettability and Pore Characteristics of Fibrous Substrates. *Polymers* **2021**, *13*, 223. [CrossRef]
61. Vallet-Regí, M.; Román, J.; Padilla, S.; Doadrio, J.C.; Gil, F.J. Bioactivity and mechanical properties of SiO2–CaO–P2O5 glassceramics. *J. Mater. Chem.* **2005**, *15*, 1353–1359. [CrossRef]
62. Xia, Z.; Yu, X.; Wei, M. Biomimetic collagen/apatite coating formation on Ti6Al4V substrates. *J. Biomed. Mater. Res.—Part B Appl. Biomater.* **2012**, *100*, 871–881. [CrossRef]
63. Belloni, A.; Argentieri, G.; Orilisi, G.; Notarstefano, V.; Giorgini, E.; D'Addazio, G.; Orsini, G.; Caputi, S.; Sinjari, B. New insights on collagen structural organization and spatial distribution around dental implants: A comparison between machined and laser-treated surfaces. *J. Transl. Med.* **2024**, *22*, 120. [CrossRef]
64. Zhao, S.F.; Jiang, Q.H.; Peel, S.; Wang, X.X.; He, F.M. Effects of magnesium-substituted nanohydroxyapatite coating on implant osseointegration. *Clin. Oral Implant. Res.* **2013**, *24* (Suppl. A100), 34–41. [CrossRef]
65. Louropoulou, A.; Slot, D.E.; Van der Weijden, F. The effects of mechanical instruments on contaminated titanium dental implant surfaces: A systematic review. *Clin. Oral Implant. Res.* **2014**, *25*, 1149–1160. [CrossRef]
66. de Tapia, B.; Valles, C.; Ribeiro-Amaral, T.; Mor, C.; Herrera, D.; Sanz, M.; Nart, J. The adjunctive effect of a titanium brush in implant surface decontamination at peri-implantitis surgical regenerative interventions: A randomized controlled clinical trial. *J. Clin. Periodontol.* **2019**, *46*, 586–596. [CrossRef]
67. Dostie, S.; Alkadi, L.T.; Owen, G.; Bi, J.; Shen, Y.; Haapasalo, M.; Larjava, H.S. Chemotherapeutic decontamination of dental implants colonized by mature multispecies oral biofilm. *J. Clin. Periodontol.* **2017**, *44*, 403–409. [CrossRef]